Comparing the accuracy of several field methods for measuring gully erosion

C. Castillo[1, *], R. Pérez[1], M. R. James[2], J. N. Quinton[2], E. V. Taguas[1], J. A. Gómez[3].

[1] University of Cordoba, Dep. of Rural Engineering, Campus Rabanales, Leonardo Da Vinci Building, 14071 Cordoba, Spain. Phone: +34-957-212-222. Fax:+34-957-218-550.

[2] Lancaster Environment Centre, Lancaster University, Lancaster, UK.

[3] Institute for Sustainable Agriculture. CSIC. Apartado 4084. 14080 Cordoba Spain.

*Corresponding author (ccastillo@uco.es)

Abstract

Most field erosion studies in agricultural areas provide little information on the probable errors involved. Here, for the first time, we compare the accuracy, time and cost of conventional and new methodologies for gully surveying, and provide a model to estimate the effort required to achieve a specified accuracy. Using a terrestrial LiDAR survey of a 7.1-m-long gully reach as a benchmark data set, the accuracies of different measurement methods (a new 3D photo-reconstruction technique, total station, laser profilemeter and pole) are assessed for estimating gully erosion at a reach scale. Based on further field measurements carried out over nine gullies (>100 m long), a simulation approach is derived to model the expected volume errors when 2D methods are used at the gully scale. All gullies considered were located near Cordoba, Spain.

At the reach scale, the field measurements using 3D photo-reconstruction and total station techniques produced cross sectional area error values smaller than 4%, with other 2D methods exceeding 10%. For volume estimation, photo-reconstruction proved similar to LiDAR data, but 2D methods generated large negative volume error (E^V) values (<-13% for laser profilemeter and pole).

We show that the proposed error expressions derived from the model are in line with the reach-scale field results. A measurement distance factor (*MDF*) is defined that represents the ratio between cross section distance and the gully length, and thus reflects relative survey effort. We calculate the required *MDF* for specified values of E^V, illustrating how *MDF* decreases with increasing gully length and sinuosity.

Abbreviations: A, cross sectional area (m^2); D, distance between adjacent cross sections (m); E^A, relative area measurement error (%); E^L, relative length error (%); E^V , relative volume measurement error (m^3); L , Gully length (m); L_{ext} , distance between the extremes of the gully (m); $L_{ext\text{-}5m}$, distance between the extremes of a 5 m reach (m); L_p, polyline length defined by cross section distance (m); L_{pol}, length of the polyline that fits coarsely the gully thalweg following knickpoints (m); $L_{real\text{-}5m}$, real length of a 5 m reach (m); *MDF*, measurement distance factor (%); n, number of sub-reaches; N_{5m}, total number of 5-m reaches within a gully; $S^{av}{}_{local}$, local sinousity; S_{gully}, gully sinuosity; *SF*, sinuosity factor; σ_{Ev} , standard deviation of the volume error distribution (%); *V*, volume of eroded soil within the gully (m^3).

Keywords: accuracy, measurement, gully, error

INTRODUCTION

Many studies have stressed the importance of gully erosion in the overall soil loss and sediment yield of agricultural catchments (e.g. Vandaele and Poesen, 1995; Valcárcel et al., 2003; Martínez-Casasnovas, 2003; De Santisteban et al., 2006; Wu et al., 2008). Finding the optimal combination of accuracy and productivity for a soil erosion assessment requires selecting the most suitable measurement method, and this will vary depending on the requirements and scale of the study. The results should then be accompanied by an appropriate estimation of the uncertainty due to measurement errors.

Gully erosion studies are performed at different spatial scales and with different goals. For example, deriving gully inventories and risk maps at region-scale (Radoane, 1995; Eustace et al., 2011), defining gully networks in small catchments at medium scale (Moges and Holden, 2008; Perroy et al., 2010), or at a small scale, to evaluate sidewall and headcut retreat rates (Wu et al., 2008; Giménez et al., 2009; Marzolff and Poesen, 2009). At the different spatial scales, measurement accuracy can be influenced differently by the morphology of the gullies. For instance, gully geometry plays an important role in determining the magnitude of the errors associated with survey work, leading to sinuosity factors being proposed to quantify the meandering characteristics of rills and gullies (Øygarden, 2003). Although broad estimations of the sinuosity influence on errors have been made (Lentz et al., 1993), no thorough analysis of this issue has been found by the authors and it has been previously noted that more work is required to provide error estimations depending on survey effort and gully morphology (Casalí et al., 2006), as well as to give guidance for determining the measurement density required to achieve a desired accuracy.

A variety of techniques are used for determining gully erosion in field studies. Conventional techniques involve the use of different devices (i.e. ruler, pole, tape, micro-topographic profilers, total station) to calculate rill and gully volumes through the determination of cross sectional areas and length of reaches (Casalí et al., 1999; Capra and Scicolone, 2002; Hessel and van Asch, 2003). Optical devices (i.e. laser profilemeters) have also been designed for the purpose of rapid and detailed measurement of cross sectional areas in gully networks (Giménez et al., 2009). These conventional 2D methods provide a simple and affordable (in terms of instrumentation) approach for erosion evaluation, but are time consuming to carry out if a good accuracy is required. Despite the fact that significant volume errors have been described even when cross sections are measured at short distance intervals (e.g. errors greater than 20%, with sections taken every 6 m using microtopographic profile meter (Casalí et al., 2006), intervals of up to 20 m for cross-sections are frequently found in studies (Capra and Scicolone, 2002; Daba et al., 2003).

Remote sensing techniques are being increasingly applied to gully erosion investigation. Traditional aerial photography and photogrammetry has been successfully used for large scale and long term investigations (e.g. Burkard and Kostaschuk, 1995; Betts and De Rose, 1999; Martínez-Casasnovas et al., 2004; Ionita, 2006) and is now being augmented by other remote technologies, such as airborne and terrestrial LiDAR (James et al., 2007; Collins et al., 2008; Evans and Lindsay, 2010). To increase resolution for assessment of short-term processes, lower altitude unmanned aerial platforms like blimps, quad-rotors or kites are starting to be used (Marzolff and Poesen, 2009; Giménez et al., 2009; Niethammer et al., 2011). Overall, new remote sensing techniques have allowed the generation of high-resolution digital elevation models (DEMs), although care must be taken to consider the effects of image resolution, the presence of vegetation and gully morphology. Consequently, surveys are usually complemented with field measurements to validate accuracies or to obtain additional details, such as cross sectional areas (Swanson et al., 1989; Giménez et al., 2009). Recently, major advances have been made in automatic 3D photo-reconstruction techniques for oblique images from un-calibrated and non-metric cameras (Snavely et al., 2006, 2007; Furukawa and Ponce, 2010). These computer vision approaches offer advantages over traditional photogrammetry techniques by making image collection and processing significantly easier, and their use has been explored in a range of studies (Dowling et al. 2009; Dandois and Ellis, 2010; Niethammer et al., 2010; Welty et al., 2010; James et al., 2011). Here, we carry out the first application of this technique for gully measurement and compare the results with established survey methods.

To the authors' knowledge, no previous studies have simultaneously compared the accuracies of a range of conventional and remote sensing techniques, or defined the most suitable method for a particular scale, given and time and cost constraints. These were the goals of the International Workshop *Innovations in the evaluation and measurement of rill and gully erosion* (Cordoba, May 2011) from which part of the material presented in this paper are derived. The main aims of this paper are to evaluate the use of different methods (terrestrial LiDAR, 3D photo-reconstruction, total station, laser profilemeter and pole) for the quantification of gully erosion at reach and gully scales, and to assess the main factors affecting the accuracy of the volume measurements. To do so, we (1) estimate the length, area and volume errors associated with these methods using a field trial at reach scale, with the LiDAR results representing the reference (i.e. zero error) data set. The trial also allows (2) a comparison of the time and cost requirements of the different techniques. At the larger, gully scale, we use field data to drive computer simulations involving large numbers of virtual gully configurations in order to (3) estimate the length errors involved in using 2D techniques, and (4) to characterise the expected volume errors and determine the critical factors that generate them. The resulting volume error model (5) can then be used to provide guidance on the survey effort required to achieve a specified accuracy, in a gully of given characteristics.

MATERIAL AND METHODS

Study areas

For the reach scale study, a 7.1-m-long gully section was chosen in an olive grove, at ‘‘La Conchuela’’ farm, 10 km west of Cordoba, Spain, (37 48′ 54′′N, 4 53′ 53′′W, Figure 1a). The reach has the following characteristics: average width-depth ratio WDR_A = 1.97, average width W_A = 2.42 m, average cross sectional area A_A = 1.84 m^2 and cross sectional area variation coefficient A_{CV} = 0.28. The site was selected because of its high sinuosity and cross-sectional area variation which would highlight accuracy variations between the different volume measurement methods.

In order to provide gully-scale field data from which computer simulations could be used to derive a volume error model, nine gullies were selected in five small catchments of the Arroyo Galapagares basin (37 49′ 9′′N, 4 35′ 39′′W, at the south-east limits of the town council of Cordoba and 20 km from the city, Fig. 1b). All sites are representative of the Campiña, a rolling landscape covered by field crops (bean, sunflower and wheat) in the Guadalquivir River Valley on, mostly, Vertisol soils under the FAO classification. The mean annual rainfall in the area is 655 mm, with 77% concentrated in the period October–March.

Determination of different error types at reach and gully scale

Figure 2 provides a visual outline of the approaches used in this paper and the error relationships derived. The errors are classified as error in length, cross-sectional area, and volume, and have been assessed from field measurements at two scales, the reach-scale, where a comparison of different measurement technologies was made, and at the gully-scale. The simulations are used to extend the reach-scale results to gully scale by generating a sufficient number of virtual scenarios so that statistical estimations of the errors can be made.

Reach scale

In order to compare the accuracy of cross sectional area determination for the five measurement techniques, three control cross sections were marked in the selected gully reach using pins and strings. Topographic data on the gully were collected using the following technologies:

- Ground-based LiDAR. Terrestrial laser scanner data were collected in the field using a Riegl model scanner (LMS-Z420i). This instrument contains a high performance long-range laser distance meter, with manufacturer specifications of 10 mm range accuracy and 4 mm average repeatability. The terrestrial scanner was considered the reference method because of its proven accuracy, high data density acquisition (up to 10 points/cm^2 over areas of multiple square metres) and general acceptance across geoscience communities. So that these data could represent a fully independent benchmark, data were collected and processed by an external commercial contractor.

To cover the complex morphology of the gully reach, the instrument had to be sited twice, with two scans acquired at each location, one with a vertical instrument orientation and the other with the scanner tilted at 60º. Retroreflectors, with coordinates determined by differential GPS (dGPS), were used for georeferencing. Raw data were processed with RISCAN PRO (Riegl) software to obtain a cleaned and merged 3D point cloud which was then interpolated into a DEM with a grid cell size of 2 cm. The outer perimeter of the gully was then delineated in the DEM, by the operator identifying the region of change in slope at the top of the gully walls. In order to compare cross section areas derived using the 2D techniques with the LiDAR data, appropriate gully cross sections were extracted from the LiDAR DEM using ISPOL civil engineer software (Istram).

- 3D photo-reconstruction: This technique, based on computer vision image-based modelling approaches (e.g. Pollefeys et al., 2004) provided a 3D reconstruction of the gully reach from photos taken with an un-calibrated and non-metric consumer digital camera (Canon EOS 450D). Under bright but overcast illumination conditions, 191 pictures were taken by hand following a walking itinerary around the gully, with six control points deployed on the gully perimeter to facilitate scaling and georeferencing of the resulting model. The relatively large number of photographs reflects the complex nature of the gully morphology and a data collection protocol aimed at minimising the likelihood of missing coverage in some area. Control point positions were determined by dGPS at the same time as the LiDAR control was established. The photo-reconstruction process was performed using the automated 'structure-from-motion' reconstruction pipeline described previously for volcanological applications (James et al., 2011), with the resulting point cloud being scaled and oriented using freely available georeferencing software (http://www.lancs.ac.uk/staff/jamesm/software/sfm_georef.htm) . The results were then interpolated over a 1 cm grid using Surfer (Golden Software Inc), and cropped to the gully perimeter determined by the LiDAR operator, to obtain a final DEM of the reach. The accuracy for the reconstruction is expected to exceed ~1:400 (Goesele et al., 2007) which, with a maximum viewing over the ~7 m spatial extent of the gully reach, corresponds to ~2 cm.

- Laser profilemeter: A laser distance meter, rotated by a stepper motor and mounted on a 2-m-long aluminium pole (Castillo et al., 2011), was used to measure cross sections in the gully. With the laser oriented orthogonal to the horizontal axis of rotation, measurements were carried out by rotating the sensor over a range of 180°, at 1.8° intervals. The pole can be horizontal (supported at either end on the gully rims) or vertical (held by the operator, guided by a bubble level indicator). In this work, with gully widths often greater than 2 m, the profilemeter was used in vertical orientation. The 100 measurements for each cross section were stored as a text file which, in conjunction with a sensor calibration to relate the soil voltage response to distance, can be converted to a cross section using a spreadsheet or drawing software tool. Five cross sections were measured (the control sections and two additional sections), with the instrument position for each being recorded by dGPS.

- Total station. Conventional cross sectional profile measurements were also carried out using a total station (Topcon GTS-210). Depending on the individual cross section complexity, a variable number of points (between 5 and 10) were taken per cross section. The same five cross sections were measured as described for the profilemeter case.

- Pole. The main gully dimensions (widths and depths) at the control cross sections were measured to estimate the cross sectional area by assuming simple geometric forms such as a triangle or trapezium (from here on, called the 'pole simplified' method). To enable further error analysis of this method following the field work, more cross sections were determined in a similar manner by using a 'virtual pole simplified' method. In this approach, appropriate width and depth dimensions are derived from the cross section profiles extracted from the LiDAR data taken at 0.1 m cross section spacings.

To derive the eroded gully volume, V, from 2D cross sectional area measurements, we use:

$$V = \sum_{i=1}^{n} V_i = \sum_{i=1}^{n} \frac{A_{i-1} + A_i}{2} \cdot D_i \qquad [1]$$

where n is the number of sub-reaches, V_i the volume of eroded soil within the sub-reach i, A_{i-1} the downstream cross sectional area of the sub-reach, A_i the upstream cross sectional area of the sub-reach and D_i the distance between adjacent cross sections.

For 3D methods (LiDAR and photo-reconstruction) gully volume was determined by subtraction of present and pre-gully elevation models estimated from the gully perimeter. Note that for the 2D methods, the gully limits were defined independently by each instrument operator, who (as part of their measurement protocol whilst in the field) identified the gully boundary by the abrupt change in slope between the gully walls and the surrounding soil surface.

Error evaluation.

In order to assess the accuracy of the cross sectional area and gully volume estimates for each method, the relative error in cross sectional area was defined:

$$E^{A} = \frac{A_p - A_o}{A_o} \times 100 \qquad [2]$$

where E^A is the relative area measurement error (%), A_p is the predicted cross sectional area (m^2) and A_o the observed cross sectional area for the reference method (m^2).

The relative error in volume estimation is similarly:

$$E^{V} = \frac{V_p - V_o}{V_o} \times 100 \qquad [3]$$

where E^V is the relative volume measurement error (%), V_p *the* predicted volume of eroded soil in the gully (m^3) and V_o the observed volume of eroded soil for reference method (m^3).

Time and cost requirements.

Time and cost estimates were made for the application of each technique, as described below:

- Time requirements for each operation (positioning, calibration, measurement and processing) were assessed at reach-scale. The results were extrapolated to a 100-m-long gully with the appropriate adaptations, e.g. by estimating the number of measurement reaches within the gully for LiDAR and photo-reconstruction (ten 10-m-long and five 20-m-long reaches were considered for LiDAR and photo-reconstruction, respectively, a reasonable hypothesis for intermediate visibility conditions) and by evaluating the number of measured cross sections required for 2D methods for different measurement densities.

- For cost analysis, both one-off costs (e.g. camera purchase) and variable costs have to be taken into account. Variable costs include rental expenses (LiDAR, total station and dGPS) and labour costs, and have been estimated from present market prices. dGPS costs are expressed independently since georeferencing is not essential for volume calculations in these methods (a measurement tape or wheel could be used to estimate the reach length in 2D techniques or to define scale for photo-reconstruction).

- The required labour resources were considered as two operators for field work for all techniques excluding photo-reconstruction which required only one, and one operator for processing.

Gully scale

A field survey was conducted in June 2011 to assess the cross sectional dimensions (width and depth) of the nine Galapagares gullies using the simplified pole method. The average distance between cross sections ranged from 10.6 m for the shortest gully (1b) to 62 m for the longest one (gully 4b). To densify the field data set, simulated cross sectional area values have been assigned at 1 m intervals between the measurement locations along each gully, using a recent orthophoto (Junta de Andalucía,

2007) to trace the route of the thalweg. These intermediate area values were generated by linear interpolation with the addition of a random component (±20% of the interpolated value) to avoid complete linear variation. Furthermore, in order to provide a wider span of reach lengths and a greater number of cases, six populations of different length reaches (i.e. L = 10, 20, 30, 40, 50 and 100 m-long reaches) were extracted from the studied gullies to carry out volume error analysis.

Volume error model.

The error model proposed in this study describes the volume error when 2D methods are used for measuring eroded gully volume. For these methods, the volume estimation for a segment of a reach is carried out by multiplying the straight line distance, D, between two bounding cross sections by the average area of the cross sections (Eq. 1). In addition to the cross section area measurement error, this approach generates two further types of errors:

- the real length of the gully is underestimated by representing its sinuous thalweg by a series of straight line segments, generating a length error E^L,
- and the average area of adjacent cross sections may poorly represent the actual mean cross sectional area of the reach, resulting in a random error in area (either positive or negative). For example, for the same number of cross sections, the same distance apart, but with a small change in the position of the sections along the gully, a different volume estimation may be obtained.

The effect of the random area error can be characterised if gully volume is calculated multiple times, for slightly different positions of the cross sections along the gully. In this case, the average volume error would tend to reflect only the systematically negative length error, E^L, and the random area error can be considered as a probabilistic distribution, with a standard deviation that could then be evaluated through the statistical analysis.

Consequently, if a normality distribution hypothesis for E^V is assumed, the volume error model can be expressed as a confidence interval:

$$E^V = E^L \pm x \cdot \sigma_{Ev} \qquad [4]$$

where x is the coefficient corresponding to a certain probability of occurrence (x = 1 for 67% probability and x = 2 for 95%) and σ_{Ev} is the standard deviation of the E^V distribution. To enable E^V confidence interval to be calculated, firstly, we use the Galapagares gullies data set to define an expression for the length error, E^L. Secondly, error variability (σ_{Ev}) is evaluated by the multiple gully simulations approach.

Length error analysis.

At the gully scale, the length error, E^L (%), affecting volumes derived from cross section area measurements, is defined by:

$$E^L = \frac{L_p - L}{L} \cdot 100 \qquad [5]$$

where L_p is the length of a polyline defined by the centres of the cross sections, and L is the length of a reference polyline along the gully thalweg defined by points 1 m apart. Consequently, E^L varies with the relationship between gully sinuosity and the distance between adjacent cross sections, D. The sinuosity of a reach is a ratio of the real length of a reach and the straight line distance between its extremes. At a gully scale, and based on field observations, gully sinuosity can be studied at two levels:

- local sinuosity ($S^{av}{}_{local}$) includes variations over scales of several meters, and is observable in the field as a zigzag morphology. Considering the length of the gullies studied (from 10 m to several hundred meters), we define a distance of 5 m as the upper limit for local sinuosity. To provide a representative value of the local winding, the local sinousity index, $S^{av}{}_{local}$, represents the average sinuosity of all 5-m-long reaches in a gully:

$$S^{av}{}_{local} = \frac{\sum_{i=1}^{N_{5m}} \frac{L_{real-5m}}{L_{ext-5m}}}{N_{5m}} \geq 1 \qquad [6]$$

where $L_{real\text{-}5m}$ is the real length of a 5 m reach (m), $L_{ext\text{-}5m}$ the distance between the extremes of a 5 m reach, N_{5m} the total number of 5-meter reaches within the gully.

- gully sinuosity (S_{gully}) takes into account the general sinuosity of a gully, excluding local sinuosity. For this purpose, the straight line distance between gully extremes can be compared with the length of a polyline that fits the gully thalweg following the major knickpoints of the meandering form of the gully (Figure 3):

$$S_{gully} = \frac{L_{pol}}{L_{ext}} \geq 1 \qquad [7]$$

where L_{pol} is the polyline length, L_{ext} is the straight line distance between the extremes of the gully and S_{gully} is the gully sinuosity index.

The second factor affecting E^L is the distance, D, between adjacent cross sections, which is related to the amount of measurement effort required. The magnitude of the relative survey effort (i.e. the number of cross sections per unit gully length) can be quantified by determining the measurement distance factor, MDF, defined as the ratio between cross section distance and gully length:

$$MDF(\%) = \frac{D}{L} \cdot 100 \qquad [8]$$

Since this index increases with decreasing measurement density (i.e. with larger values of D for any particular L), it represents an inverse indicator of the relative survey effort.

The sinuosity factors of the nine gullies data set have been assessed. For each reach extracted from the gullies data, E^L was determined for increasing D (D =2, 3, 4, 5, 10, 20, 30, 40, 50 and 100 m, for $D < L$). The length error component of the volume error model was then determined by applying multivariate regression analysis to the resulting E^L values as a function of MDF, S^{av}_{local} and S_{gully}.

Assessment of the volume error variability.

For variability analysis of volume error, a generalised stochastic experiment was made through simulations in ActionScript 2.0 (Adobe). With volume error variability not being a function of gully length, only one gully was required to provide initial measurements for the simulations, and gully 1a was selected because of its intermediate length, average cross sectional area and variation coefficient (Table 4). Volume error variability, σ_{Ev}, was then determined using the methodology described below (Figure 4):

1. A set of 50 simulated gullies were generated by assigning cross sectional area values at the same locations as the field measurements in gully 1a. The measured cross sectional area measurements from gully 1a did not fit a common statistical distribution (normal and lognormal), so, for each simulation, area values were randomly selected from a uniform distribution that spanned the interval of measured values from gully 1a.

2. Additional cross sectional area values were added to each virtual gully using the interpolation process previously described (see the start of the *Gully scale* section).

3. Volume error values were determined for each L-m-long reach using the same series of measurement spacings as in length error analysis, and with the reference volume (i.e. zero error) defined by that calculated for the minimum measurement distance, D = 1 m.

4. The normality hypothesis for the volume error distributions was confirmed through normality tests. The random component of E^V was then estimated for each combination of *MDF* and reach length, by calculating the standard deviations σ_{Ev} for each appropriate volume error population.

5. A regression analysis was then carried out to derive an expression for σ_{Ev} as a function of *MDF*.

The performance of the error model was tested by applying it to the reach-scale field study. Cross sections were extracted from the LiDAR data set at various separation distances, and used to estimate gully volumes for different values of D. Associated E^L and E^V confidence interval values were predicted, and the results compared with the actual gully volume, as determined from the full LiDAR DEM.

Finally, the expression derived for the E^V confidence interval was solved (using Engineering Equation Solver 2008, F-chart Software) for fixed relative errors using a wide range of gully lengths and sinuosities. This enables expressions for the required *MDF* values for a given accuracy to be determined by multivariable regression.

RESULTS AND DISCUSSION

Reach scale

Cross sectional area error assessment

In Figure 5, cross sectional profiles, area values and E^A values for the three control sections of the reach-scale field site are shown. The lowest relative errors occurred, as expected, with the 3D photo-reconstruction method, with an $\left|E^A\right|$ average value of 1.9%. For the total station data, the average error was 2%, a lower value than may be expected given the limited point density within cross sections (<10), but one that reflects the operator skill in selecting appropriate measurements to best represent the profile.

The laser profilemeter data show a clear tendency to underestimate cross sectional areas. This method had an average error of -9.9%, with a maximum approaching -15% at the first section. Although the general shape of the cross sections fits well to LiDAR results, the data appear to be affected by a systematic scale error. Among other minor causes of error, we consider that the use of the sensor in motion could introduce a voltage offset, since the previous field calibration was performed with the sensor in static position. The profilemeter measurement protocol includes the auxiliary determination of the top gully width with a measurement tape, to provide later control for the results. When these data are compared, an approximate distance error of 10 cm has been found for the three control sections. If the profilemeter data are corrected by this magnitude, the cross sectional area values become 1.78, 1.48 and 3.27 m^2 for sections 1 to 3 respectively, representing errors of -4.8%, 1.4% and -2.7% when compared with LiDAR results. Further research is required to assess such calibration issues, which probably reflect sensitivity of the instrument response to voltage offsets and to other factors as variations in ambient light, differences in texture and color of soil surfaces.

Finally, the simplified pole approach produced the greatest errors, reaching -23.5%, with an average of -10.9%. The negative bias in the errors reflects a tendency for area underestimation by this technique. This was confirmed by comparing the areas of further cross sections extracted from the LiDAR with those predicted by the virtual pole simplified method. In 73% of cases E^A is negative (-10.7% average error) and in

27%, overestimation occurred (5% average error). Thus, negative cross sectional area errors are greater and more frequent than positive values when the pole simplified method is used.

For all methods, the estimation of the boundary position between the gully and the undisturbed surface generates an uncertainty factor for the area and volume calculation. For the total station and pole simplified techniques, this estimation is carried out in the field and is implicit within the first and last measurement of each profile. For the LiDAR, photo-reconstruction and profilemeter methods, this decision is carried out during data processing, with the aid of drawing or 3D point cloud processing software. Comparison of the boundary estimates made for the different techniques did not show significant differences, although, with the well differentiated channel-bank morphologies of the reach studied, it could be argued that this site did not represent a very stringent test. For a method comparison that excludes variability in gully boundary estimates, it would be necessary to deploy field bench marks that explicitly define the limits of the cross sections, and this is suggested for further studies.

Volume error evaluation

The volume assessment results are shown in Table 1. The method that produced the best approximation to the LiDAR value was photo-reconstruction, with a low E^V value of -3.1%. Total station error remains positive and below 7%, whereas laser profilemeter and virtual pole errors exceeded the -13% level.

The elevation differences between the DEMs generated with LiDAR and photo-reconstruction can be seen in Fig. 6. Most areas show differences less than 3 cm (grey zone), with larger positive differences around the gully rims (black zone, with a maximum of 15 cm) and negative in the north west corner where the reconstruction was somewhat incomplete (white zone). Most anomalies are thought to represent areas where the techniques differed in their handling of near-vertical surfaces complicated by protruding roots and overhanging vegetation. The anomalies in north west corner stem from a complex of intertwined roots and leaves that prevented surface reconstruction by the photo technique, but did provide laser returns (although not necessarily from the soil surface). The large positive anomaly on the west gully wall reflects the fact that this area, which was reconstructed by the photo-method, was not imaged by the LiDAR due to being occluded by the complex topography from both scanner locations.

For the total station data, E^V was positive and exceeded 6%. This represents a combination of the three defined errors, E^A, E^L and the random area error; because E^A was low (2%) and E^L systematic and negative, the random cross sectional area error must dominate to produce the positive E^V value. This was confirmed using sections extracted from the LiDAR data at 0.1 m intervals along the reach (Fig. 7). For this particular section of the gully, the average of the five sections´ areas exceeds the mean cross sectional area, resulting in a positive E^V for the total station data.

For the laser profilemeter and pole simplified methods, E^V was large and negative (-13.3 and -15.3% respectively). These methods underestimated gully volumes because the strongly negative E^A values (e.g. Fig. 5) dominated the random cross sectional area error. Overall, the results indicate that 2D methods can produce significant volume errors, even when relatively short distances between cross sections are used (e.g. an average 1.44 m, corresponding to five sections over a 7.1 m reach). This is in line with previous studies which show that a cross sectional distance between 1 and 3 m is needed to guarantee volume errors less than 10% for gullies 14 and 30 m long (Casalí et al., 2006).

The influence of cross sectional distance on volume estimation

In order to assess the influence of cross section distance on volume errors, with no influence from area measurement errors, analysis was performed using cross sections extracted from the reference LiDAR data (Table 2). For $D < 1$ m, errors were small and negative (less than - 4%), but an increasing positive error was produced as *D* increased. For $D = 7.1$ m ($MDF = 100\%$) the error exceeds 30%. As cross sectional density reduces, the bounding cross sections increase their influence in the overall volume calculation which, for the gully reach studied, produced overestimation (Fig. 7).

The results show that even the best 2D method for cross sectional area determination (total station), carried out at short cross section spacings (i.e. <1.5 m, corresponding to a MDF=20%), can produce high volume errors at reach scale. Thus, the expected E^V depends more on relative measurement density (expressed inversely by *MDF*) than on absolute spacing *D*. The relationship between E^V and *MDF* is explored at the gully-scale approach.

Time and cost requirements

Table 3 shows the time and cost requirements for the five techniques at reach scale, and equivalent estimates for a gully 100 m long. The most expensive method is LiDAR, at about ten times the cost of 3D photo-reconstruction. Photo-reconstruction costs are the same order of magnitude as 2D methods. If a high density measurement is required ($MDF < 3\%$), photo-reconstruction performs more economically than profilemeter. Additional cost evaluations showed that even LiDAR acquisition turns out to be more inexpensive than 2D methods at very short spacings ($D < 0.3$ m). Thus, there will be intervals of suitability for different methods depending on the measurement requirements, but photo-reconstruction provides good accuracy and cost for both of the assessed scenarios. At the present costs, LiDAR would be an expensive tool for common gully erosion projects, although it may be applicable for validation purposes. Profilemeter has a span of suitability covering medium levels of accuracy in gully networks evaluations, whereas the pole simplified method is the most inexpensive tool, but suitable mainly for coarse gully volume estimations at large scale. From these results, it may be inferred that the advantages associated with using a total station are outweighed by its disadvantages when compared with the other evaluated methods.

Gully scale

Length error analysis

Table 4 shows the calculated local and gully sinuosity factors for the nine studied gullies. S^{av}_{local} varies less than S_{gully}, because of its local scope (5 m) and average nature. In Figure 8, length error is shown as a function of D for each of the nine complete gullies and, with the exception of gully 1a (which had the maximum S^{av}_{local} value), length error remains under 10%, even for minimum survey effort. Regression analysis provides:

$$E^{L}(\%) = -0.228 \cdot L^{0.484} \cdot \left(MDF(\%)^{0.361} \right) \cdot {S^{av}_{local}}^{5.15} \cdot S_{gully}^{\left(\frac{56.12}{L}\right)} \quad (\,n{=}221,\ R^{2} = 0.744) \quad [9]$$

with MDF being the variable that explains the highest proportion of the variance. As the survey effort decreases (i.e. fewer cross sections, with correspondingly increased MDF), errors increase. As expected, local sinuosity plays an important role in E^L (reflected by its large exponent), whereas the impact of gully sinuosity reduces as L increases. For L > 10 m, local sinuosity exerts more influence than gully sinuosity. These results suggest that gully sinuosity has a major influence on length errors in very short gullies, but becomes less significant for longer gullies. On the other hand, errors tend to increase with gully length, because the direct influence of length on E^L exceeds its mitigating effect on gully sinuosity (due to the latter is very close to 1). Thus, for long gullies, *MDF* must be decreased if length error magnitudes are to be maintained, suggesting that a scale factor is important when considering the measurement uncertainty in gullies.

To simplify the results further, the influence of sinuosity can be given as a sinuosity factor (*SF*) derived from the regression analysis (Table 4):

$$SF = {S_{local}^{av}}^{5.15} \cdot S_{gully}^{\left(\frac{56.12}{L}\right)} \qquad [10]$$

Since the sinuosity indexes are key factors determining the expected magnitude of the errors, to plan measurement effort for a field survey, they must be estimated in advance (e.g. from orthophotos or topographic maps). As in other disciplines, a preliminary evaluation is required in order to optimise the collection of appropriate data.

Equation 9 represents an attempt to develop a general approach to cover a wide range of sinuosities and gully sizes but, strictly, this and the following equations express the relationships observed only in the sample of gullies used. Although the equations are likely to be applicable to other gullies within the landscape from which they were derived, for different environments they should be used only for first estimates (in the absence of a better reference), and as parameterisations to refine through local calibration.

Assessment of the volume error variability

Table 5 shows the characteristics of the simulation process carried out to assess the variability of volume error. A large number of virtual gully configurations have been analysed for each reach length with a maximum of 2,400 for $L \approx 10$ m and a minimum of 200 for $L \approx 100$ m. A_{cv} distribution parameters of the simulated data (mean of 0.307

and maximum of 0.516) are close to those determined for areal variability found in field surveys by other authors (e.g. Casalí et al. (2006) obtained A_{cv} values ranging from 0.27 to 0.43 for five gullies ranging from 14 to 30 m long in Navarra). However, as shown in Table 4, gully 1a, from which the field measurements were taken for the simulations approach, presents a medium value for A_{cv} if compared to the remainder of Galapagares gullies. This could mean that E^V variability is underestimated for gullies with a high cross sectional variability.

The average and standard deviation of E^V for the simulation samples, for each D and L values, have been used to define the confidence interval for a certain probability (Fig. 9). The results show that the E^V confidence interval widens with increasing D, but narrows with increasing L, and is biased toward negative values (because E^L is systematically negative). Using regression, an estimate for σ_{Ev} can be derived:

$$\sigma_{Ev} = 3.2 \cdot \left(MDF(\%)\right)^{0.41} \qquad \textit{(n=45, } R^2 = 0.953\textit{)} \qquad [11]$$

Consequently, expressing the volume error model as an E^V confidence interval for 67 and 95% probabilities gives:

$$E^V_{67\%} = -0.228 \cdot L^{0.484} \cdot MDF(\%)^{0.361} \cdot SF \pm 3.2 \cdot MDF(\%)^{0.41} \ [12]$$

$$E^V_{95\%} = -0.228 \cdot L^{0.484} \cdot MDF(\%)^{0.361} \cdot SF \pm 2 \cdot 3.2 \cdot MDF(\%)^{0.41} \ [13]$$

Thus, given the sinuosity factor and the length of the gully to be evaluated for a chosen field effort, the E^V confidence interval can be determined. Hence, field measurements can now be used to provide an estimate of soil eroded volume that is bounded by expected upper and lower limits.

If the real length between sections is assessed in the field (e.g. by deploying a measuring tape at the gully thalweg or by using a measuring wheel) the length error influence would be removed. The E^V confidence interval would then be defined by the standard deviation component alone, it would not be negatively biased and the maximum expected errors would be reduced. Required *MDF* values can be directly evaluated by solving the E^V confidence interval equations. For 67% probability, and desired errors of 10 and 20%, *MDF* values of 16.1 and 87.3% are required respectively; to increase to 95% probability for the same errors, *MDF* values would need to be reduced to 3.0 and 16.1%.

Testing the volume error model at reach scale

For the reach-scale field site, sinuosities were $S^{av}{}_{local}$ = 1.075, S_{gully} = 1.052 and *SF*=2.17, giving the predicted E^L, σ_{Ev} and E^V confidence interval values (equations 9, 11 and 12) shown in Table 6.

The predicted E^L value (-6.68%) is suitably similar to the observed length error (-8.31%) for D = 7.1 m, to be considered an acceptable result, taking into account that this case corresponds to the lower extreme of gully size range. Furthermore, observed E^V value*s* obtained by LiDAR remain inside the predicted 67% confidence interval, with the exception of D = 7.1 that exceeds the higher limit. This is a consequence of the coincidence of bounding sections with the maximum values of cross sectional areas within the reach, an eventuality with a low occurrence probability. Note that, for all cases, the predicted volume confidence interval included the measured value for soil eroded volume by the LiDAR (13.29 m^3).

The model performance has proven to be satisfactory at reach scale. Additionally, the model provided good results predicting the confidence interval of volume errors when applied to the nine gullies data set at gully scale. However, full validation of the model would require a supplementary gully dataset and, just as for the

E^L analysis, the model validity for other geographic regions has not been determined and is left for future work.

Field effort design for a desired error limit

Regression analysis applied to the solutions of the E^V confidence interval expressions (Eq. 12 and 13), showed that *MDF* can be expressed as a function of the target $\left|E^V\right|$, *L* and *SF*:

$$MDF(\%)_{(67\%\,probab)} = 0.065 \cdot \frac{\left|E^v(\%)\right|^{2.5}}{L^{0.1} \cdot SF^{0.2}} \qquad (n=630,\ R^2 = 0.995) \qquad [14]$$

$$MDF(\%)_{(95\%\,probab)} = 0.01 \cdot \frac{\left|E^v(\%)\right|^{2.5}}{L^{0.05} \cdot SF^{0.1}} \qquad (n=630,\ R^2 = 0.998) \qquad [15]$$

The volume error magnitude, $\left|E^V\right|$, has a major influence over the *MDF* value, (with an exponent of 2.5), and has inverse relationships with both *SF* and *L*. Thus, a higher relative survey effort is required for long and sinuous gullies.

Evaluating the expressions for two fixed error values (10 and 20%) and for different gully lengths and sinuosities, gives the results in Table 7. For instance, for *SF* = 1.5 (a value close to the average sinuosity factor of the simulations) and a 67% probability of achieving an error magnitude of <10% for short gullies (e.g. *L* = 10 m), *D* must be less than 1.5 m (*MDF* = 15.1%). For longer gullies (e.g. *L* = 200 m), a cross section distance of 22 m (*MDF* = 11.2%) is required to achieve the same error magnitude. If the confidence level for the volume estimate is raised to 95% probability, *MDF* remains close to 2.5% with little variation due to sinuosity and gully length. If an error limit of $\left|E^V\right|$< 20% is required (at 95% probability), then the necessary *MDF* (~14%) represents a significant reduction in measurement distance. Considering the reach scale study, to guarantee a probable error of <10%, a 1 m cross section distance (MDF = 14.2% for $L \approx 10$ m and $SF \approx 2$) would be required to achieve a 67% probability, but a 0.18 m cross section distance would be needed for 95% probability (MDF = 2.6%). This demonstrates that a significant survey effort is required in order to reduce error probability.

CONCLUSIONS

This paper has focused on error evaluation when measuring gully erosion at different scales. The comparison between 2D and 3D methods has showed the superiority of the 3D techniques for obtaining accurate cross sectional data, with the results from some commonly used 2D methods subject to systematic errors. In particular, the pole simplified method has showed a clear tendency to underestimate area. Laser profilemeter results suggest that further research on calibrating optical devices for a variety of soil conditions must be carried out to improve its performance.

For volume estimations, photo-reconstruction results provided an excellent approximation to terrestrial laser data and we have demonstrated that this new remote sensing technique has a promising field application in soil erosion studies. In contrast, using 2D approaches resulted in significant error, even over short measurement distances. However, if cost and time requirements are considered as well as accuracy, then a 2D method may still be an optimum approach for large scale studies.

The simulations demonstrated that the accuracy of 2D methods for volume estimation depends greatly on the gully morphology and measurement density. The relative survey effort, given by measurement distance factor (MDF), had a major influence on length errors as well as on volume error variability.

The volume error model derived from the simulations may be applied for two purposes: firstly, to design a field survey that should satisfy a required maximum error and, secondly, to determine the confidence interval of the volume estimate once the survey has been completed. In the first case, sinuosity factors must be estimated in a preliminary study to obtain the required *MDF*. In the second, sinuosity factors can be calculated from the field measurements.

Volume error confidence interval expressions have been proposed for 67 and 95% probabilities. The volume error model performed well in estimating probable errors at reach scale, but should be further validated across a wider range of gully conditions as well as in other geographic contexts.

Regarding field effort level results, *MDF* decreased with gully length and sinuosity. For 95% probability, *MDF* remains approximately constant at ~2.5% and ~13% for E^V values of <10% and <20% respectively.

For gully conditions similar to those from which the expressions were derived our errors estimations can be directly applied for survey planning and design, enabling optimal survey effort for a specified accuracy to be determined in advance,. They also provide a first estimation of errors, and a methodology for calibrating the error expressions to other geographic regions and environments based on local field measurements.

ACKNOWLEDGEMENTS

This study was supported by Projects P08-AGR-03925 (Andalusian Government) and AGL2009-12936-C03-01 (Spanish Ministry of Science and Innovation), RESEL (Spanish Ministry for Environment and Rural and Marine Affairs) and FEDER funds. This support is gratefully acknowledged. We are also very grateful to Francisco Natera the owner of the farm “La Conchuela” and their staff for their support and to

Metrocuadrado Topografía S.L. for their technical assistance with LiDAR data acquisition and cost analysis.

REFERENCES

Betts H.D., and R.C. DeRose. 1999. Digital elevation models as a tool for monitoring and measuring gully erosion. International Journal of Applied Earth Observation and Geoinformation 1: 91–101.

Burkard, M.B. and R.A. Kostaschuk. 1995. Initiation and evolution of gullies along the shoreline of Lake Huron. Geomorphology 14: 211-219.

Capra, A., and B. Scicolone. 2002. Ephemeral gully erosion in a wheat cultivated area in Sicily (Italy). Biosystems Engineering 83(1): 119–126.

Casalí, J., J.J. López and J.V.Giráldez, 1999. Ephemeral gully erosion in southern Navarra (Spain). Catena 36: 65– 84.

Casalí, J., J. Loizu, M.A.Campo, L.M. De Santisteban and J. Álvarez-Mozos. 2006. Accuracy of methods for field assessment of rill and ephemeral gully erosion. Catena 67: 128–138.

Castillo, C., Giráldez, J.V., Gómez, J.A., Liñán, M., Peña, A. and Taguas, E. 2011. Patent: Perfilómetro portátil medidor de cárcavas mediante láser y control por microprocesador. Ref: P201131055. University of Cordoba and IAS-CSIC.

Collins, B.D., K.B. Brown and H.C. Fairley. 2008. Evaluation of terrestrial LIDAR for monitoring geomorphic change at archeological sites in Grand Canyon National Park, Arizona. U.S. Geological Survey Open-File Report 2008-1384.

Daba, S., W. Rieger and P. Strauss. 2003. Assessment of gully erosion in eastern Ethiopia using photogrammetric techniques. Catena 50: 273–291.

Dandois, J. P., and E. C. Ellis. 2010. Remote sensing of vegetation structure using computer vision. Remote Sensing.2: 1157-1176, doi: 10.3390/rs2041157.

De Santisteban, L.M., J. Casalí and J. J. López. 2006. Assessing soil erosion rates in cultivated areas of Navarre (Spain). Earth Surface Processes and Landforms 31: 487–506.

Eustace, A.H., M.J. Pringle and R.J. Denham. 2011. A risk map for gully locations in central Queensland, Australia. European Journal of Soil Science 62 : 431–441.

Evans, M., and J. Lindsay. 2010. Quantifying gully erosion in upland peatlands at the landscape scale. Earth Surface Processes and Landforms 35:876–886.

Dowling, T. I., A. M. Read, and J. C. Gallant. 2009. Very high resolution DEM acquisition at low cost using a digital camera and free software, in 18th World IMACS/MODSIM09 International Congress on Modelling and Simulation, edited, pp. 2479-2485.

Furukawa, Y., B. Curless, S. M. Seitz, and R. Szeliski. 2010.Towards internet-scale multi-view stereo, in IEEE Conf. Comp. Vis. Pattern Recog., pp. 1434-1441.

Furukawa Y. and J. Ponce. 2010. Accurate, dense, and robust multiview stereopsis. IEEE Trans Pattern Anal Mach Intell 32(8):1362–1376.

Giménez, R., I. Marzolff, M. A. Campo, M. Seeger, J. B. Ries, J. Casalí and J. Álvarez-Mozos. 2009. Accuracy of high-resolution photogrammetric measurements of gullies with contrasting morphology. Earth Surface Processes and Landforms, 34(14): 1915-1926.

Goesele, M., N. Snavely, B. Curless, H. Hoppe and S.M. Seitz. 2007. Multi-view stereo for community photo collections. Proc Int Conf Comp Vis. doi: 0.1109/ICCV.2007.4408933.

Hessel, R., and T. van Asch. 2003. Modelling gully erosion for a small catchment on the Chinese Loess Plateau. Catena 54: 131-146.

Ionita, I. 2006. Gully development in the Moldavian Plateau of Romania. Catena 68: 133-140.

James, L.A., D.G. Watson and W.F. Hansen. 2007. Using LiDAR data to map gullies and headwater streams under forest canopy: South Carolina, USA. Catena 71: 132–144.

James, M. R., L.J. Applegarth and H. Pinkerton. 2011. Lava channel roofing, overflows, breaches and switching: insights from the 2008-9 eruption of Mt. Etna. Bull. Volc., doi: 10.1007/s00445-011-0513-9.

Junta de Andalucía, Consejería de Medio Ambiente. 2007. Available at http://www.juntadeandalucia.es/medioambiente/site/rediam/menuitem.aedc2250f6db83cf8ca78ca731525ea0/?vgnextoid=0863d61d8470f210VgnVCM2000000624e50aRCRD&lr=lang_es

Lentz, R.D., R.H. Dowdy and R.H. Rust. 1993. Soil property patterns and topographic parameters associated with ephemeral gully erosion. Journal of Soil and Water Conservation 48 (4): 354– 361.

Martínez-Casasnovas, J.A. 2003. A spatial information technology approach for the mapping and quantification of gully erosion. Catena 50: 293–308.

Martínez-Casasnovas, J.A. 2003. A spatial information technology approach for the mapping and quantification of gully erosion. Catena 50: 293– 308.

Martínez-Casasnovas, J.A., M.C. Ramos and J. Poesen. 2004. Assessment of sidewall erosion in large gullies using multi-temporal DEMs and logistic regression analysis. Geomorphology 58: 305–321.

Marzolff, I., and J. Poesen. 2009. The potential of 3D gully monitoring with GIS using high-resolution aerial photography and a digital photogrammetry system. Geomorphology 111: 48–60.

Moges, A., and N.M. Holden. 2008. Estimating the rate and consequences of gully development, a case study of Umbulo catchment in southern Ethiopia. Land Degradation and Development 19: 574–586.

Niethammer, U. S. Rothmund , M. R. James, J. Travelletti, M. Joswig. 2010. UAV-based remote sensing of landslides, Int. Arch. Photgrammetry, Rem. Sens. Spatial Info. Sci, Vol XXXVIII, Part 5, Comm. V Symp. Newcastle upon Tyne, U.K. p 496-501.

Niethammer, U., M.R. James, S. Rothmund, J. Travelletti and M. Joswig. 2011. UAV-based remote sensing of the Super-Sauze landslide: Evaluation and results. Engineering. Geology, doi:10.1016/j.enggeo.2011.03.012

Øygarden, L. 2003. Rill and gully development during an extreme winter runoff event in Norway. Catena 50: 217–242.

Perroy, R.L., B. Bookhagen, G. Asner, and O. Chadwick. 2010. Comparison of gully erosion estimates using airborne and ground-based LiDAR on Santa Cruz Island, California. Geomorphology 118: 288-300.

Pollefeys, M., L. V. Gool, M. Vergauwen, F. Verbiest, K. Cornelis, J. Tops, and R. Koch. 2004. Visual modeling with a hand-held camera. Int. J. Comp. Vis. 59: 207-232.

Radoane, M., I. Ichim and N. Radoane. 1995. Gully distribution and development in Moldavia, Romania. Catena 24: 127–146.

Snavely, N., S. M. Seitz, and R. Szeliski. 2006. Photo tourism: Exploring photo collections in 3D. ACM Trans. Graphics, 25: 835-846.

Snavely, N., S.M. Seitz, R. Szeliski. 2007. Modeling the world from internet photo collections. Int J Comp 422 Vis 80(2):189–210.

Swanson, M. L., G. M. Kondolf, and P. J. Boison. 1989. An example of rapid gully initiation and extension by subsurface erosion, coastal San Mateo County, California. Geomorphology 2 : 393-403.

Valcárcel, M., M.T. Taboada, A. Paz and J. Dafonte. 2003. Ephemeral gully erosion in northwestern Spain. Catena 50: 199–216.

Vandaele, K., and J. Poesen. 1995. Spatial and temporal patterns of soil erosion rates in an agricultural catchment, central Belgium. Catena 25 : 213– 226.

Welty, E., W. T. Pfeffer, and Y. Ahn. 2010. Something for everyone: Quantifying evolving (glacial) landscapes with your camera, in Fall Meeting, A.G.U., Abstract IN33B-1314.

Wu, Y., Q. Zheng, Y. Zhang, B. Liu, H. Cheng, and Y. Wang. 2008. Development of gullies and sediment production in the black soil region of northeastern China. Geomorphology 101: 683–691.

Table 1. Soil eroded volume (*V*) and volume relative errors (E^V) for all the methods.

Method	*V* (m3)	E^V(%)
LiDAR	13.29	--
Photo-reconstruction	12.88	-3.1%
Laser profilemeter	11.52	-13.3%
Total station	14.14	6.4%
Pole simplified	11.25	-15.3%

Table 2. Soil eroded volume (*V*) and volume relative errors (E^V) as a function of cross section distance (*D*) for the reference method (LiDAR).

D (m)	*V (m^3)*	E^V *(%)*
0.1	13.29	0.00%
0.5	12.99	-2.26%
1.0	12.82	-3.54%
2.0	14.00	5.34%
2.3	14.30	7.60%
3.5	14.29	7.52%
7.1	17.31	30.25%

Table 3. Time and cost requirements for the five methods at reach and 100 m scale. *MDF*: measurement distance factor. Times at the reach scale are given per 3D model (lidar and photo-reconstruction) or per cross section (profilemeter, total station and pole). † Field costs include positioning, calibration and measurement expenses.‡ Georeferencing costs only are applicable when a fully georeferenced model is needed.

Time and cost requirements for the five methods for 100 m-long gully					
One-off instrument costs ($)	Rental	656 (camera)	2,625	Rental	Negligible
***MDF* = 1%**	**LiDAR**	**Photo-reconstruction**	**Profilemeter**	**Total station**	**Pole**
Unitary Field Time (min/m)	8.3	1.3	3.1	5.5	2.0
Unitary Process time(min/m)	12.0	3.0	7.0	5.0	3.0
Unitary total Time (min/m)	**20.3**	**4.3**	**10.1**	**10.5**	**5.0**
Field costs † ($)	4,174	55	273	782	177
Georeferencing costs ‡ ($)	907	137	341	601	221
Process costs ($)	525	131	306	219	131
Total costs ($)	**5,607**	**323**	**920**	**1,602**	**529**
Cost per meter ($/m)	**56.1**	**3.2**	**9.2**	**16.0**	**5.3**
***MDF* = 2.5%**					
Unitary Field Time (min/m)	8.3	1.3	1.3	2.5	0.8
Unitary Process time(min/m)	12.0	3.0	2.8	2.0	1.2
Unitary total Time (min/m)	**20.3**	**4.3**	**4.1**	**4.5**	**2.0**
Field costs ($)	4,174	55	115	355	72
Georeferencing costs ($)	907	137	144	273	90
Process costs ($)	525	131	122	87	52
Total costs ($)	**5,607**	**323**	**382**	**716**	**214**
Cost per meter ($/m)	**56.1**	**3.2**	**3.8**	**7.2**	**2.1**
***MDF* = 5%**					
Unitary Field Time (min/m)	8.3	1.3	0.7	1.5	0.4
Unitary Process time(min/m)	12.0	3.0	1.4	1.0	0.6
Unitary total Time (min/m)	**20.3**	**4.3**	**2.1**	**2.5**	**1.0**
Field costs ($)	4,174	55	63	213	37
Georeferencing costs ($)	907	137	79	164	46
Process costs ($)	525	131	61	44	26
Total costs ($)	**5,607**	**323**	**203**	**421**	**109**
Cost per meter ($/m)	**56.1**	**3.2**	**2.0**	**4.2**	**1.1**

Table 4. Characteristics of the studied gullies. †D_{av} : average distance between adjacent cross sections; A_{av}: average crosss sectional area; A_{cv}: cross sectional area variation coeffcient; L_{real} : real gully length; L_{pol}: length of the coarse-fit polyline following knickpoints; L_{ext}: straight distance between extremes of the gully; S^{av}_{local}: local sinuosity; S_{gully}: gully sinuosity; *SF*: sinuosity factor

Gully name	†D_{av} (m)	A_{av} (m^2)	A_{cv} (%)	L_{real} (m)	L_{pol} (m)	L_{ext} (m)	S^{av}_{local}	S_{gully}	*SF*
Galapagares 1a	11.3	11.6	46.9	553.6	503.0	468.3	1.052	1.074	1.307
Galapagares 1b	10.6	13.2	54.7	212.7	206.0	203.1	1.035	1.014	1.197
Galapagares 2a	30.1	6.0	69.4	422.1	411.0	352.1	1.026	1.167	1.162
Galapagares 2b	40.9	6.2	38.0	735.7	689.0	611.7	1.034	1.126	1.201
Galapagares 3a	31.2	8.1	82.8	438.0	417.1	400.7	1.036	1.041	1.206
Galapagares 3b	31.3	3.9	36.9	407.8	395.1	382.3	1.024	1.034	1.135
Galapagares 4a	30.5	4.2	66.9	762.6	737.2	694.7	1.027	1.061	1.150
Galapagares 4b	62.0	4.0	104.6	1,488.2	1,413.0	1,144.5	1.024	1.235	1.141
Galapagares 5	27.4	6.8	77.8	465.5	446.4	419.5	1.025	1.064	1.142

Table 5. Characteristics of the simulation process observations. †A_{cv}: areal variation coefficient; $S^{av}{}_{local}$: local sinuosity; S_{gully}: gully sinuosity; *SF*: sinuosity factor

Gully length *L* (m)	10 m	20 m	30 m	40 m	50 m	100 m
Number of simulated gullies	2,400	1,200	800	600	480	200
A_{CV} † distribution	*Mean* = 0.307; *Std. Dev.* = 0.067; *Max* = 0.516; *Min* = 0.002					
$S^{av}{}_{local}$ distribution	*Mean* = 1.044; *Std. Dev.* = 0.010; *Max* = 1.056; *Min* = 1.012					
S_{gully} distribution	*Mean* = 1.063; *Std. Dev.* = 0.051; *Max* = 1.235; *Min* = 1.002					
***SF* distribution**	*Mean* = 1.590; *Std. Dev.* = 0.480; *Max* = 3.726; *Min* = 1.086					

Table 6. Comparison of observed errors and probable error estimations using cross sections extracted from LiDAR data at reach scale. † *D*: distance between extracted cross sections (m); *Obs. V*: Soil eroded volume value calculated using the cross sections (m^3); *Obs.* E^L: Relative length error value (%); *Pred.* E^L: Expected relative length error value using Eq. 9 (%); *Obs* E^V: Volume error calculated for the *Obs. V* values with respect to the absolute reference volume (13.29 m^3) determined by the full LiDAR data set (%); σ_{Ev}: Expected standard deviation value using Eq. 11 (%); E^V *confidence interval*: Expected relative volume error confidence interval using Eq. 12; *Pred. V interval*: Expected soil eroded volume confidence interval (m^3), derived by applying E^V confidence interval to measured volume, *Obs.V*.

***D*† (m)**	***Obs. V* (m^3)**	***Obs.* E^L (%)**	***Pred.* E^L (%)**	***Obs.* E^V (%)**	**σ_{Ev} (%)**	**E^V *confidence interval (67%)***	***Pred. V interval* (m^3) *(67%)***
0.5	12.99	-0.99	-2.51	-2.26%	6.92	(4.41, -9.42) %	11.77-13.56
1.0	12.82	-2.25	-3.29	-3.54%	9.42	(6.13, -12.72) %	11.19-13.61
2.0	14	-2.40	-4.24	5.34%	12.57	(8.33, -16.82) %	11.65-15.17
2.3	14.3	-3.92	-4.46	7.60%	13.31	(8.85, -17.77) %	11.76-15.56
3.5	14.29	-3.82	-5.18	7.52%	15.75	(10.57, -20.93) %	11.30-15.80
7.1	17.31	-8.31	-6.68	30.25%	21.05	(14.37, -27.73) %	12.51-19.80

Table 7. *MDF*† as a function of *L* and *SF* for fixed 10% and 20% E^V values considering 67% and 95% probability. *MDF*: measurement distance factor (%); *L:* gully length (m); *SF*: sinuosity factor; E^V: relative volume error (%)

10% Volume Relative error (67% probability)					*10% Volume Relative error (95% probability)*				
SF	***L*=10**	***L*=50**	***L*=100**	***L*=200**	***SF***	***L*=10**	***L*=50**	***L*=100**	***L*=200**
1.1	16.0%	13.6%	12.7%	11.9%	**1.1**	2.8%	2.6%	2.5%	2.4%
1.5	15.1%	12.8%	12.0%	11.2%	**1.5**	2.7%	2.5%	2.4%	2.3%
2	14.2%	12.1%	11.3%	10.5%	**2**	2.6%	2.4%	2.3%	2.3%
3	13.1%	11.2%	10.4%	9.7%	**3**	2.5%	2.3%	1.6%	1.1%
20% Volume Relative error (67% probability)					*20% Volume Relative error (95% probability)*				
SF	***L*=10**	***L*=50**	***L*=100**	***L*=200**	***SF***	***L*=10**	***L*=50**	***L*=100**	***L*=200**
1.1	90.6%	77.1%	72.0%	67.2%	**1.1**	15.8%	14.6%	14.1%	13.6%
1.5	85.2%	72.5%	67.7%	63.1%	**1.5**	15.3%	14.1%	13.6%	13.2%
2	80.4%	68.5%	63.9%	59.6%	**2**	14.9%	13.7%	13.3%	12.8%
3	74.1%	63.1%	58.9%	54.9%	**3**	14.3%	13.2%	12.7%	12.3%

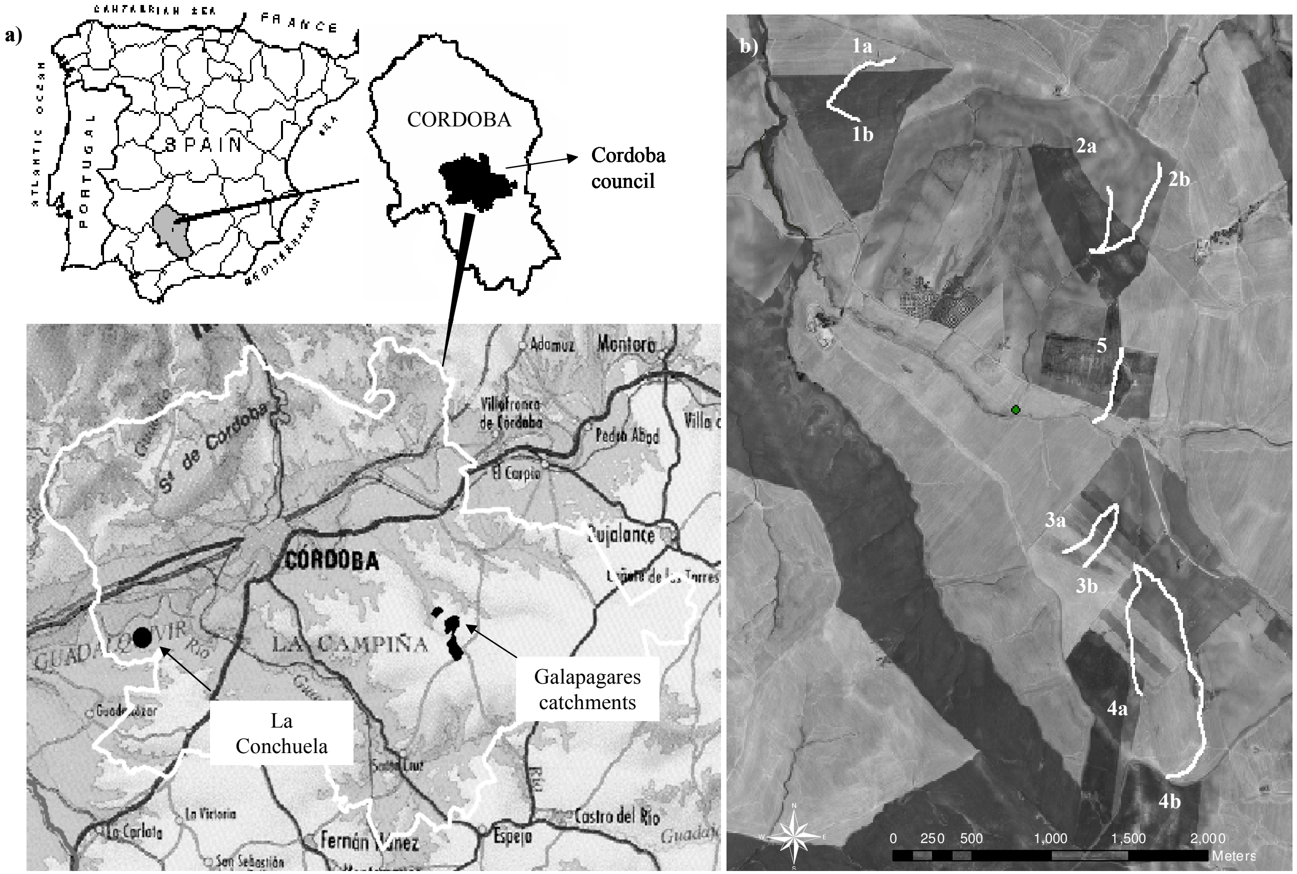

Figure 1. a) Study sites location; b) Aerial view of studied gullies

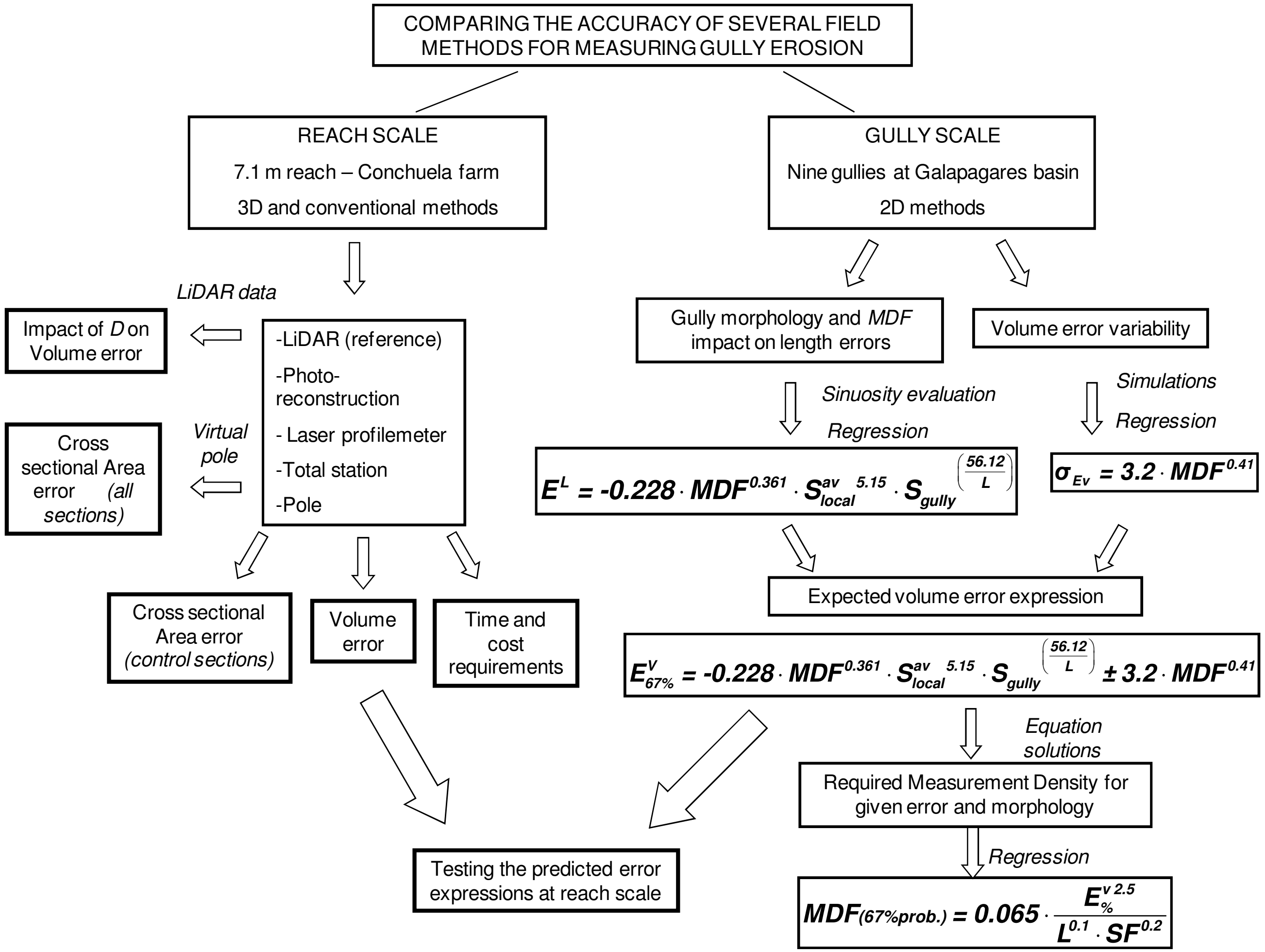

Figure 2. Diagram of the followed methodology.
MDF: measurement distance factor; *L:* gully length (m); $S^{av}{}_{local}$: local sinuosity; S_{gully} : gully sinuosity; *SF*: sinuosity factor; E^L = relative length error (%); E^v = relative volume error (%) ; σ_{Ev}: volume error standard deviation (%).

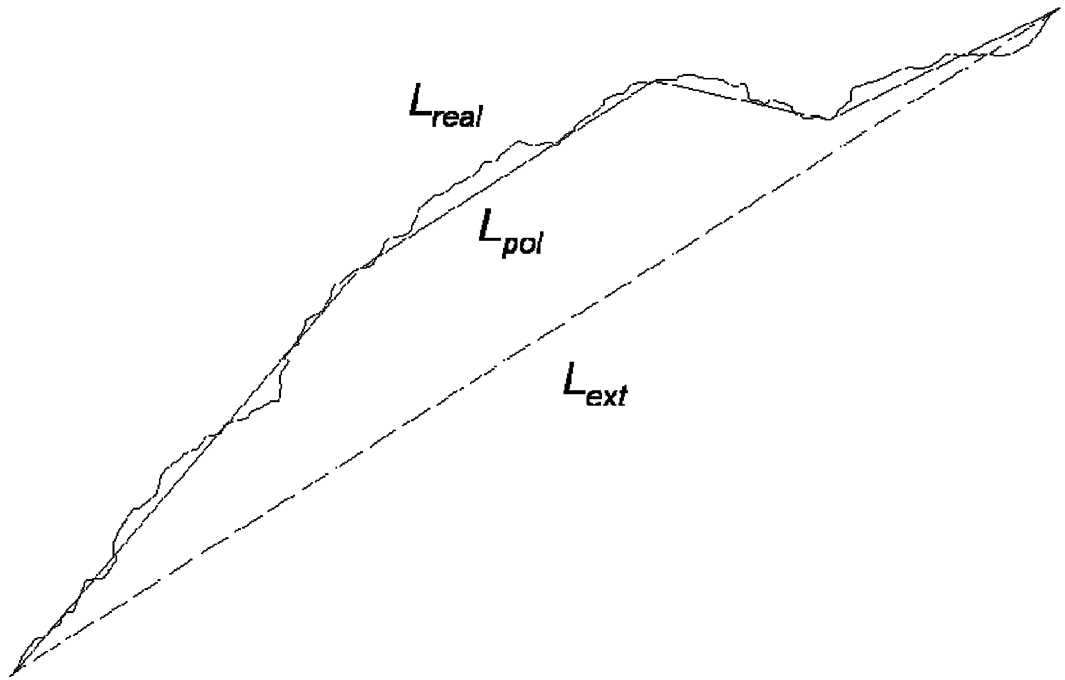

Figure 3. Differences between real length (L_{real} -irregular continuous line), coarse-fit polyline (L_{pol} – continuous line) and extremes length (L_{ext} – dashed line) at gully "1a" for defining S_{gully}.

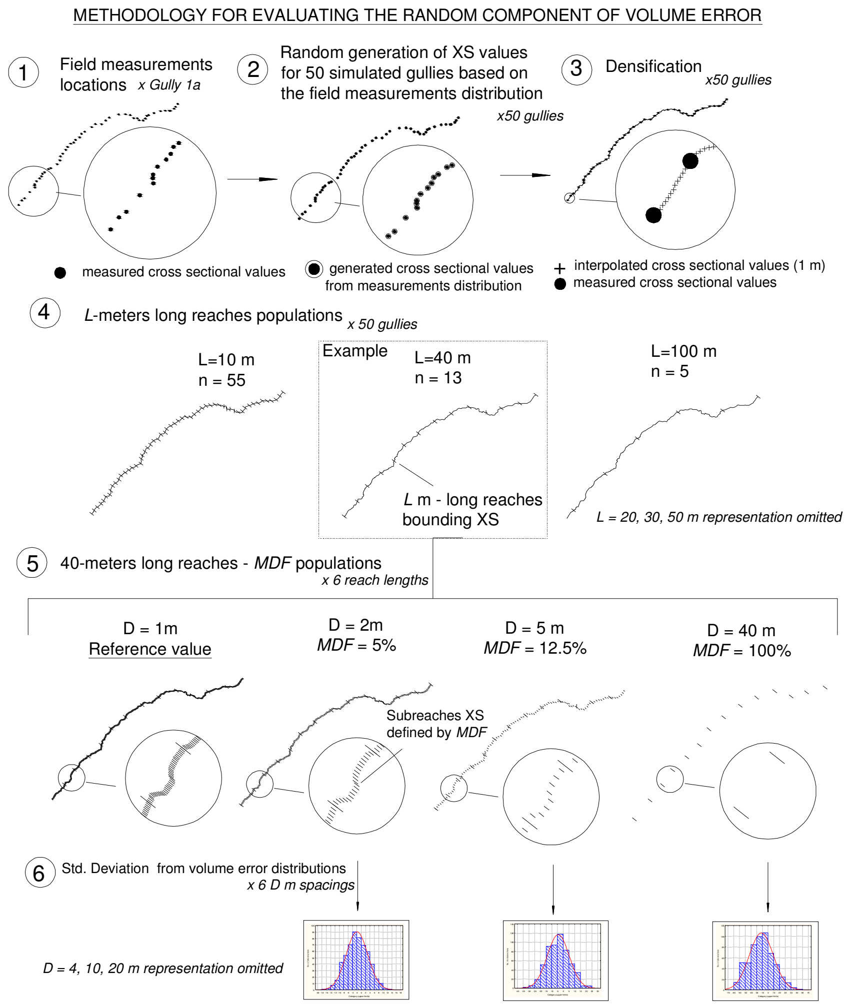

Figure 4. Methodology for the evaluation of the random component of the volume error.
D: distance between cross sections (m); *MDF*: measurement distance factor; *L:* reach length (m); σ_{Ev} *:* volume error standard deviation (%).

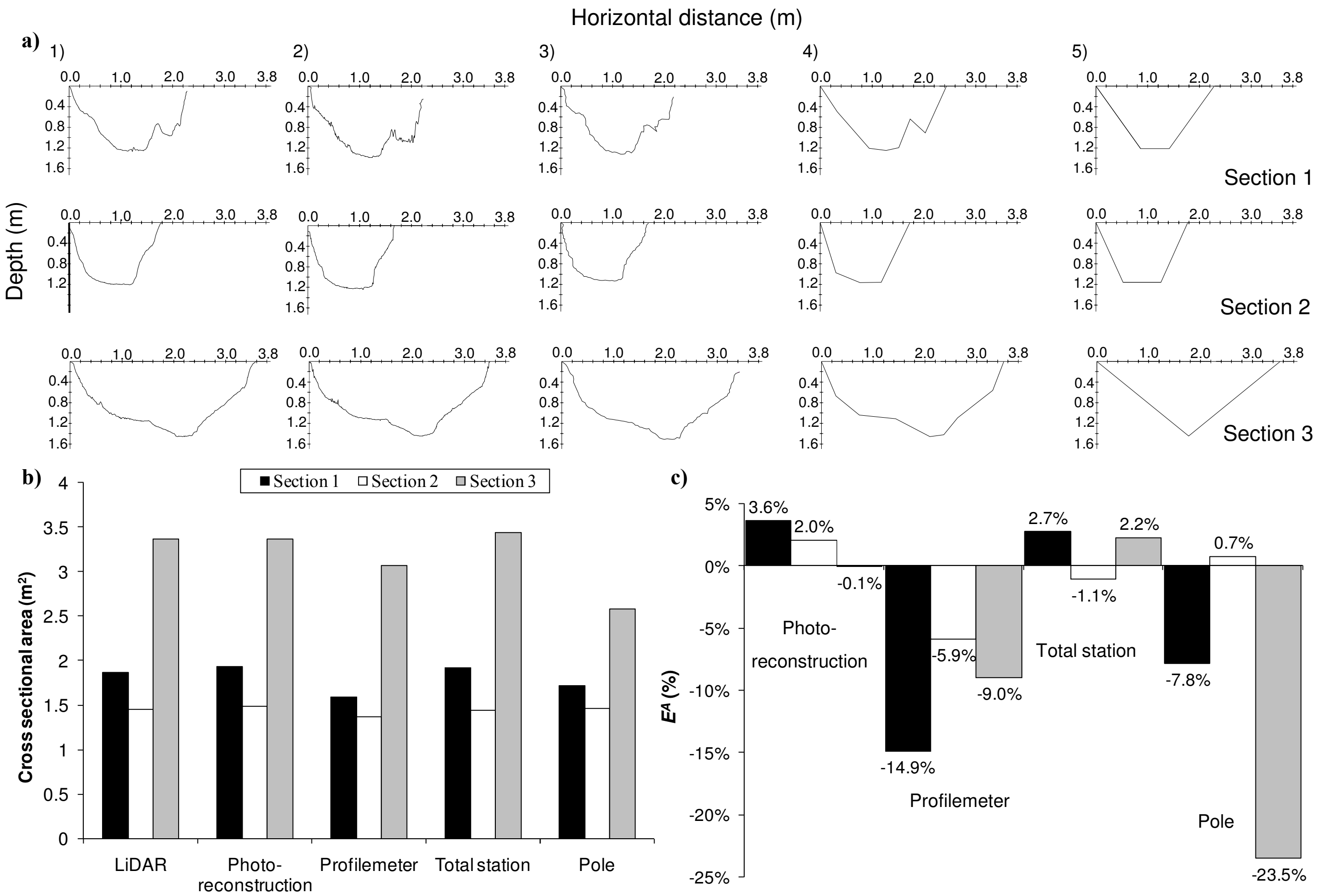

Fig. 5. a) Control cross sections profiles obtained by the five methods: 1-LiDAR, 2-Photo-reconstruction, 3- Laser profilemeter, 4 -Total station, 5-Pole; b) cross sectional area values and c) relative cross sectional error (E^A) in the three control sections.

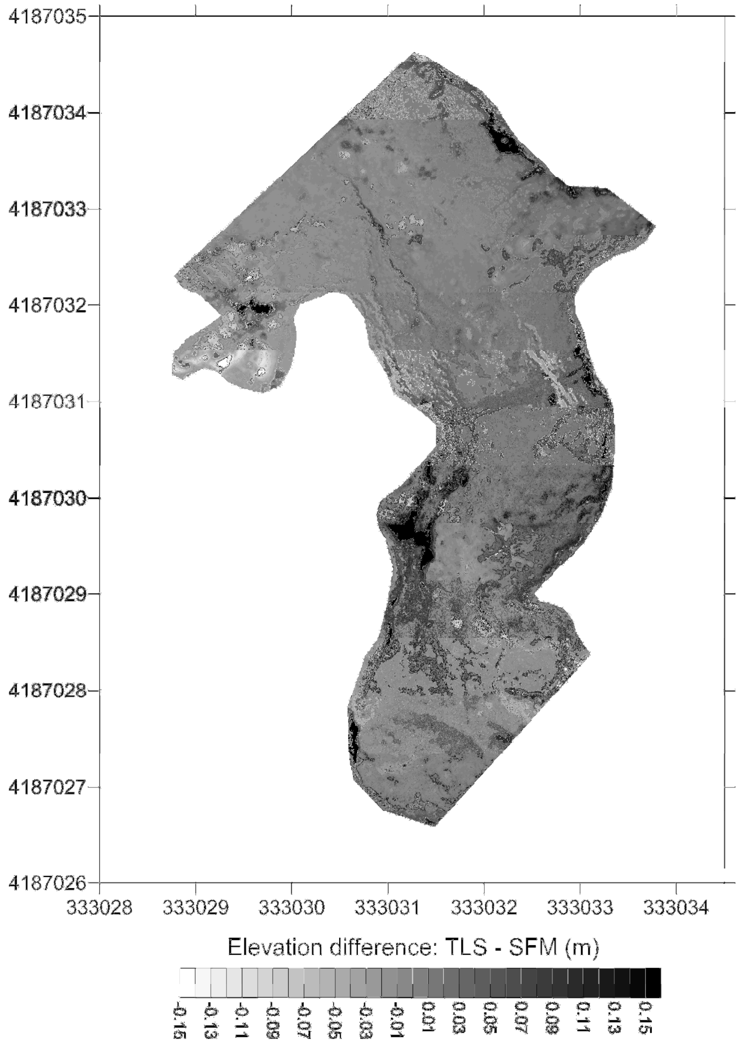

Figure 6. Elevation differences between terrestrial laser (TLS) and stucture-from-motion based photoreconstruction (SFM) in meters.

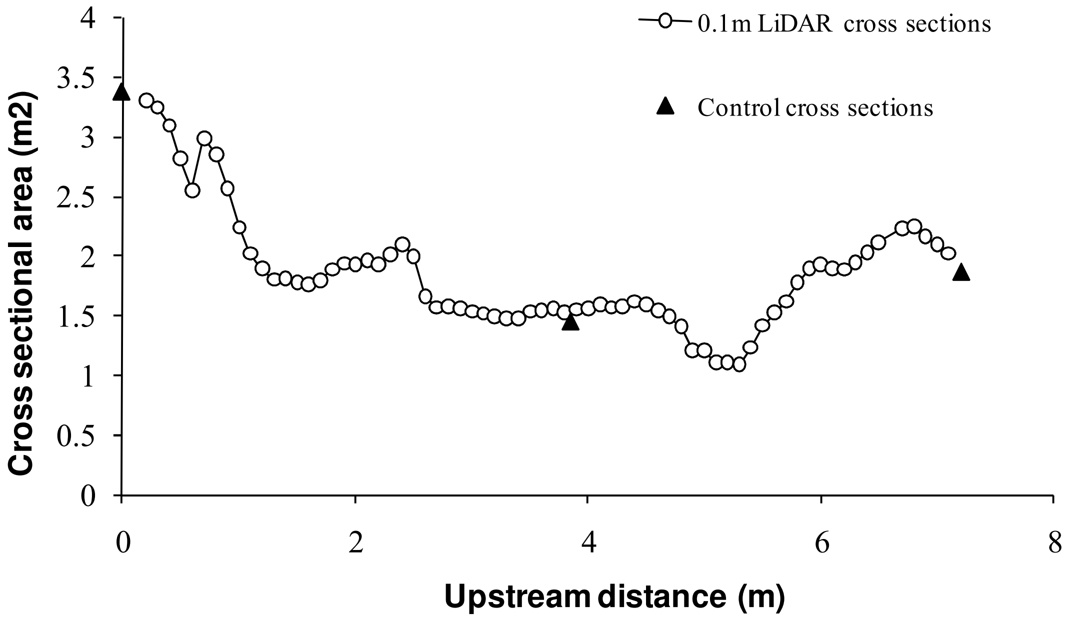

Fig. 7. Cross sectional area of the reach as a a function of upstream distance. Control control sections values are shown in triangles.

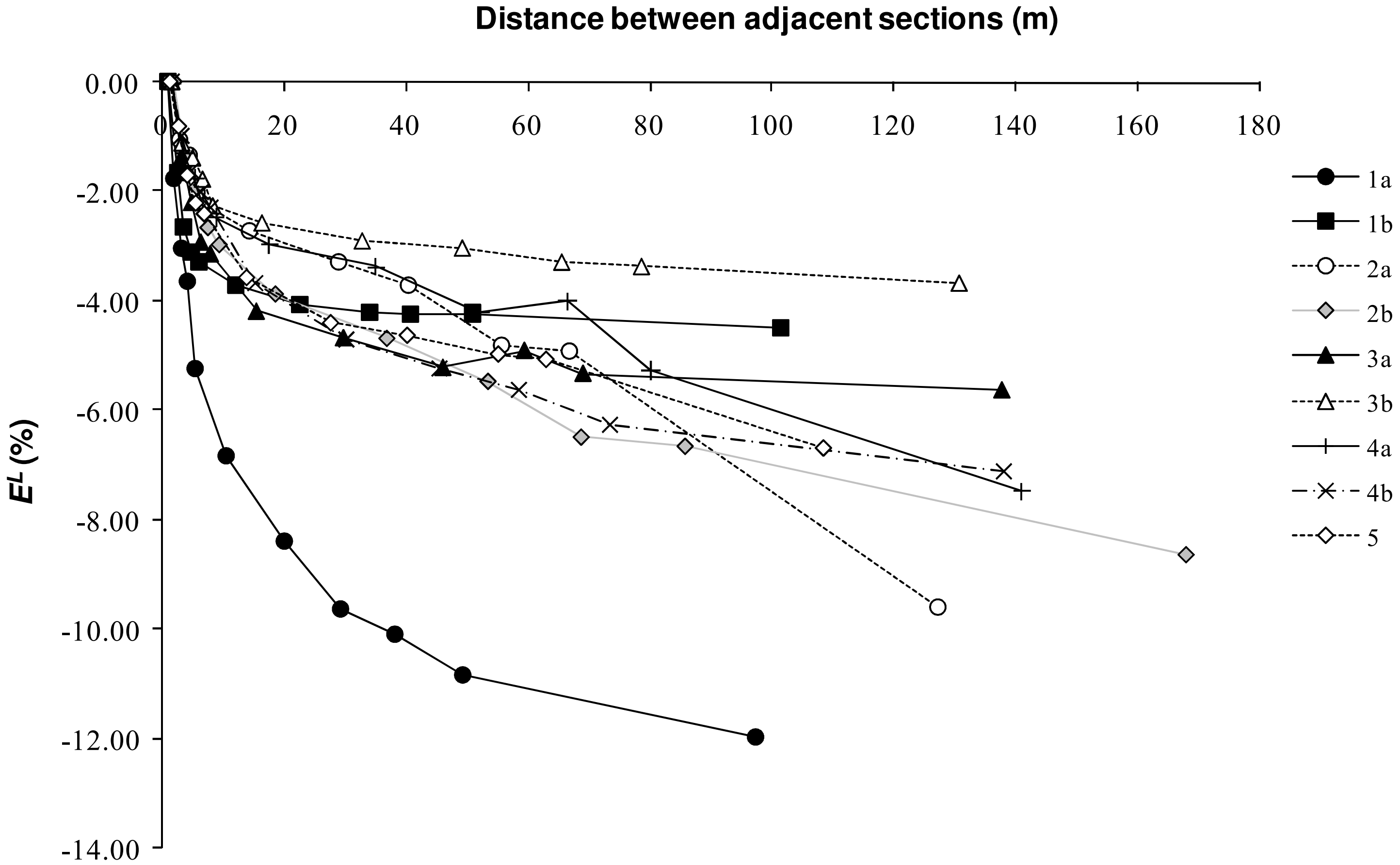

Fig. 8. Relative length error (E^L) as a function of cross sectional distance between sections (D) at the nine Galapagares gullies.

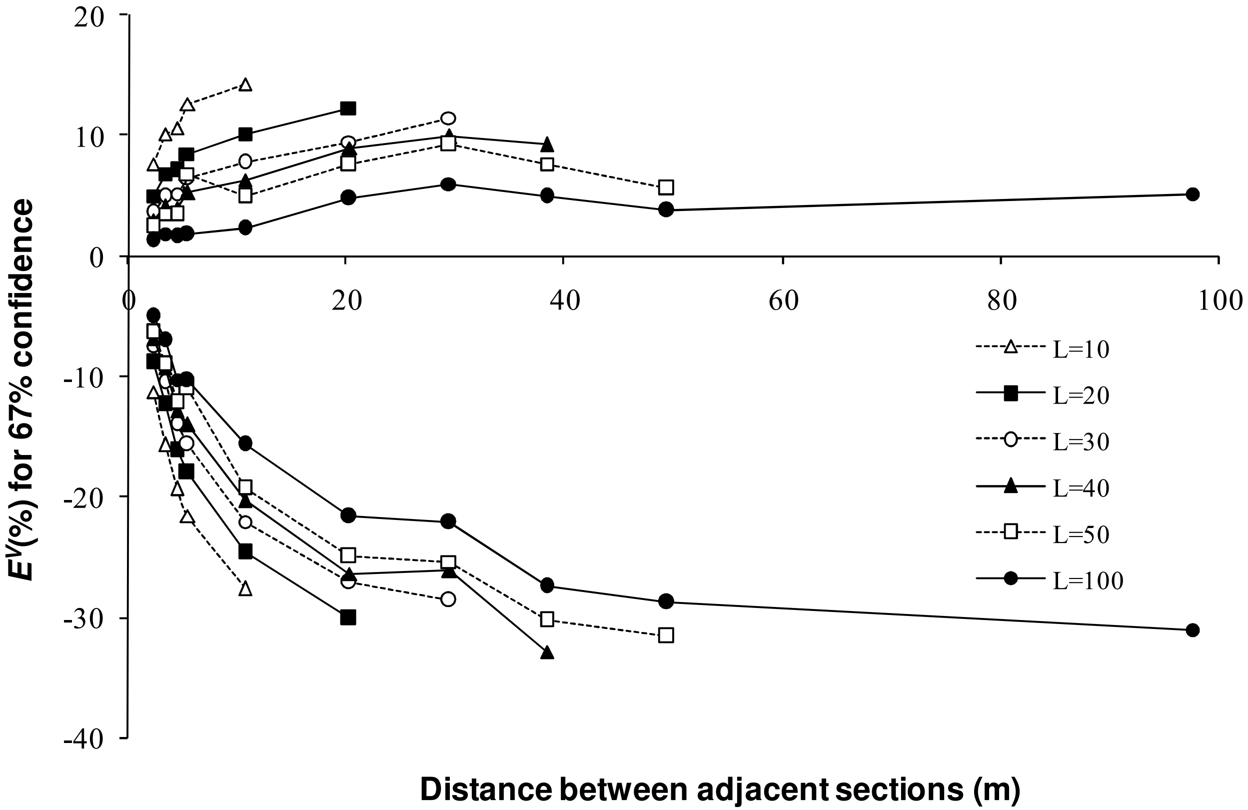

Fig. 9. Relative volume error E^V confidence interval for 67% probability as a function of cross sectional distance between sections *(D)* and gully length (*L)* obtained in the simulation process.